The Role of Atmosphere on Phase Transformations and Magnetic Properties of Ulvospinel

Catherine Groschner[1], Song Lan[1], Adam Wise[1], Alex Leary[1], Matthew S. Lucas[2], Changyong Park[3], David E. Laughlin[1], Marina Diaz-Michelena[1,4], and Michael E. McHenry[1]

[1]Materials Science and Engineering Department, Carnegie Mellon University, Pittsburgh, PA 15213 USA
[2]Air Force Research Laboratory, Wright-Patterson AFB, OH 45433 USA
[3]High Pressure Collaborative Access Team, Geophysical Laboratory, Carnegie Institution of Washington, Argonne, IL 60439 USA
[4]Space Programs and Space Sciences Department, Instituto Nacional de Técnica Aeroespacial, 28850 Madrid, Spain

We have synthesized the antiferromagnetic mineral ulvospinel, Fe_2TiO_4, in Ar to assess the role of inert atmosphere on phase formation and magnetic properties. We report the role of atmosphere on a possible phase transition and the magnetic properties of this mineral. Atmosphere dependent transformations of ulvospinel are observed with increasing temperature. Oxidation of ulvospinel to form metastable titanomaghemite is shown to occur at 300 °C in atmospheric conditions. Only slight titanomaghematitzation was observed in samples transformed under pressure in *in situ* temperature dependent X-ray experiments. Formation of ilmenite and hematite from ulvospinel was observed under high temperature, high pressure, and low oxygen atmosphere conditions.

Index Terms—Martian mineral, remnant magnetization, thermal magnetic property, titanomagnetite.

I. INTRODUCTION

THE PSEUDOBINARY titanomagnetites, $xFe_2TiO_4 - (1 - x)Fe_3O_4$, are magnetic spinels where fine microstructures influence extrinsic magnetic properties. They are a common magnetic mineral on the earth [1], the moon [2], and Mars [3]. The magnetic characteristics of these minerals contribute to planetary field anomalies and gives clues to geomagnetic evolution [4]. These minerals' contribution to regions of remnant magnetization observed on the Martian surface argues for their importance in magnetic surveying efforts of the surface [5]. The occurrence of spinodal decomposition in titanomagnetites may help explain large remnant magnetizations. We have presented evidence [8], [9] for spinodal decomposition in magnetite (Fe_3O_4)-rich titanomagnetite solutions $(x < 0.5)$ and studied structural, magnetic, and thermal properties in solid solutions across the series and identified cation distributions by Mossbauer spectroscopy [10]. Our end goal is to understand titanomagnetites, but it is critical to understand the magnetic properties and possible transitions of ulvospinel first, since it is an end member of the pseudo-binary system and may be a phase present in spinodally decomposed titanomagnetite.

Néel temperatures in titanomagnetites vary linearly with composition. The Néel temperature of ulvospinel rich solutions $(x > 0.5)$ fall in the day to night temperature swing of Mars, suggesting that identification of minerals on the Martian surface is possible with magnetic sensors based on their temperature dependent magnetization. Phase equilibria in oxidizing, inert, and reducing environments may impact the remnant state of the minerals in planetary environments.
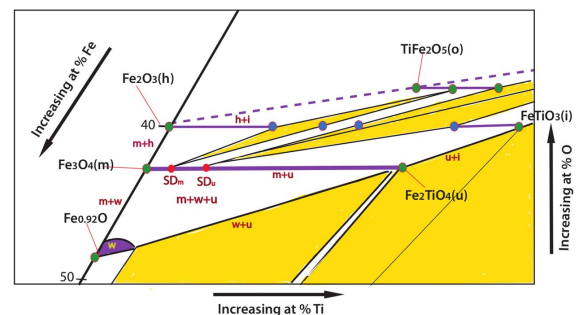
Fig. 1. Portion of the reported ternary Fe-Ti-O phase diagram at 700 °C showing the titanomagnetite and ilmenite hematite pseudo-binaries. m = magnetite; o = orthorhombic $TiFe_2O_5$; u = ulvospinel; h = hematite; i = ilmenite and w = wustite [11].

Fig. 1 is a section of the ternary Fe-Ti-O phase diagram at 700 °C, which includes the titanomagnetite and ilmenite-hematite pseudo-binaries [11]. Lamellar structures exsolved from a cooled ilmenite-hematite solid solution have been postulated as responsible for remanence dominated planetary magnetic field anomalies [12], while others suggest spinodal decomposition in magnetite-rich titanomagnetites [6] as responsible. Recent work [10] showed charge localization in ulvospinel-rich titanomagnetites. The composition dependence of the magnetic dipole moments, $m(x)$, in this system can deviate from a rule of mixtures [13]. The ground state model for $m(x)$ proposed by Néel [14] changes slope at the $x = 0.5$ composition, suggesting cation ordering may occur at this composition in which case, like the titanohematites, a second miscibility gap may occur in the $x > 0.5$ region. It is important, however, to distinguish between exsolved spinel structures and metastable structures, not reported on equilibrium phase diagrams, resulting from oxygen or cation deficiencies, as seen in maghemites [15].

In Ti-rich $(x > 0.5)$ titanomagnetites, exsolution can give rise to fine microstructures and thus peak broadening in XRD measurements. We report on solid solutions, exsolution

processes and magnetic properties of these compounds in a companion paper [16]. Though exsolution cannot occur in end-member ulvospinel, peak broadening was observed. The origin of this peak broadening is of interest and we study the role of atmosphere on its observation here.

II. EXPERIMENTAL PROCEDURES

Ulvospinel was synthesized from stoichiometric mixtures of hematite and anatase with 3 at% excess Fe sponge. Precursors were ball milled for 10 min before wet grinding in acetone. Pellets were prepared using a uniaxial press. Pellets were sintered in Ar for 72 h. The composition of the pellets was confirmed by X-ray diffraction (XRD).

Ulvospinel samples were used in three experiments. In the first, the sample was ground, placed in a ceramic crucible, and heated in air in a box furnace at $300\,^{\circ}\mathrm{C}$ for 1 h. In the second, the sample was crushed into chunks, placed in a fused quartz tube, and encapsulated in Ar by evacuating the quartz tube using a vacuum pump, filling it with Ar and repeating the process four times before filling the tube with Ar to 5 mmHg. Encapsulated samples were heated in a box furnace at $300\,^{\circ}\mathrm{C}$ for 2.5 h. In the third experiment, the sample was encapsulated in Ar in the same manner and heated to $650\,^{\circ}\mathrm{C}$ for 2.5 h. Annealed samples were analyzed by XRD and scans were compared to the scans of as synthesized samples to assess peak broadening. Peaks were deconvoluted and the full-width half-maximum (FWHM) values were calculated with a peak analysis package in Igor Pro.

High pressure and temperature energy dispersive XRD measurements were performed with the HPCAT 16-BM-B beamline at the Argonne National Lab Advanced Photon Source (APS). An ulvospinel powder sample was placed in a Paris–Edinburgh press (Model VX3) cell assembly that can generate pressures of up to 10 GPa and temperatures to $20000\,^{\circ}\mathrm{C}$ during *in situ* XRD. Parallel white-beam XRD has an energy range of 5–120 keV and the maximum diffraction angle, 2θ, is 40°. For our measurement, the diffraction angle was 8°. A Type K thermocouple (chromel/alumel) wire and a Au foil standard were placed near the sample. Au foil was used to calibrate pressure and refine the diffraction angle by matching the lattice parameter of Au at room temperature. The pressure and refined 2θ by Au marker was 649.78 MPa and 7.992°. A custom sample gasket assembly with a BN pressure medium in a graphite heating element surrounded by an MgO holder was used. Collimation insured the majority of detected intensity was from the sample, though some BN peaks were present in diffraction patterns.

III. RESULTS AND DISCUSSION

Fig. 2(a) shows that XRD patterns of samples annealed in Ar coincide with those of unannealed ulvospinel. The air annealed sample shows marked peak broadening compared to the unannealed sample and a large change in FWHM after heating. Ulvospinel, as the end member of the titanomagnetite pseudo-binary system, cannot undergo an exsolution process, therefore another process is responsible for the observed peak broadening. Ulvospinel encapsulated in Ar exhibits little additional peak broadening; any broadening observed cannot be distinguished from instrumental peak broadening. This indicates the mechanism responsible for peak broadening in air-annealed samples
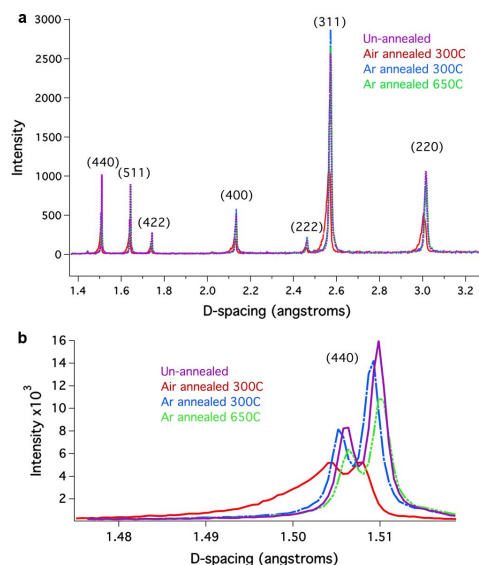

Fig. 2. (a) XRD of as synthesized, air-annealed, and in argon annealed ulvospinel samples. (b) Broadening of (440) spinel peak. XRD performed using Cu $\mathrm{K}\alpha_1$ radiation high angle peaks exhibiting $\mathrm{K}\alpha_1$ and $\mathrm{K}\alpha_2$ splitting.

is atmosphere dependent. Fig. 2(b) shows the relative broadening of the (440) peak under different atmospheres, note that the double peak structure reflect the Cu $\mathrm{K}\alpha_1$ Cu $\mathrm{K}\alpha_2$ splitting.

Peak broadening in air-annealed samples extend to the left of the original peak in plots of intensity versus d-spacing. This suggests a second phase forms with a spinel peak pattern similar to ulvospinel but at lower d-spacing due to a smaller lattice constant. As shown in Fig. 3(a), two peak patterns overlap and account for the broadening to lower d-spacing. Igor Pro was used to deconvolute overlapping peaks in the XRD pattern from the air-annealed sample. The peaks match peaks corresponding to ulvospinel and maghemite. This suggests that the air-annealed sample had oxidized and began the process of titanomaghematization, a process where titanomagnetites oxidize to form metastable titanomaghemite [15]. The oxidation process accounts for the difference in peak broadening, as encapsulated samples do not oxidize.

Deconvolution of the (440) peak of the air annealed sample is shown in Fig. 3(a) and the (440) peak of the Ar annealed at $650\,^{\circ}\mathrm{C}$ sample is shown in Fig. 3(b), both done in Igor Pro. The top plot shows the residual, the middle graph the experimental data in green with the calculated peak as the dotted blue line, and the bottom plot shows the peaks required to simulate the observed peak. a) On the left, peaks labeled 0 and 1 in the bottom plot correlate to the $\mathrm{K}\alpha2$ and $\mathrm{K}\alpha1$ (440) peak of maghemite while 2 and 3 correlate to the $\mathrm{K}\alpha2$ and $\mathrm{K}\alpha1$ (440) peak of ulvospinel. b) $\mathrm{K}\alpha2$ and $\mathrm{K}\alpha1$ split peaks are required to fit the data. The complexity of this fitting motivates single wavelength synchrotron experiments below.

Evidence for the formation of titanomaghemite is also observed in the magnetization data of Fig. 4(a). Magnetization in spinel ferrites depends on the cation disorder [17], [18]. Properties studies of the titanomagnetite and titanomaghemite pseudobinaries have produced conflicting results [19]–[22]. In Fig. 4(a), the sudden increase and then decrease in magnetization between $300\,^{\circ}\mathrm{C}$ to $550\,^{\circ}\mathrm{C}$ suggests the formation
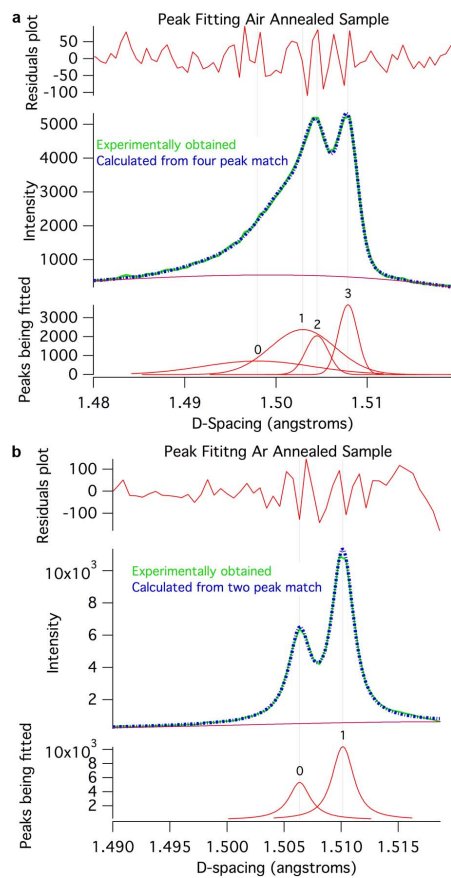
Fig. 3. (a) Deconvolution of the (440) peak of the air annealed sample and (b) Ar annealed sample at 650 °C.
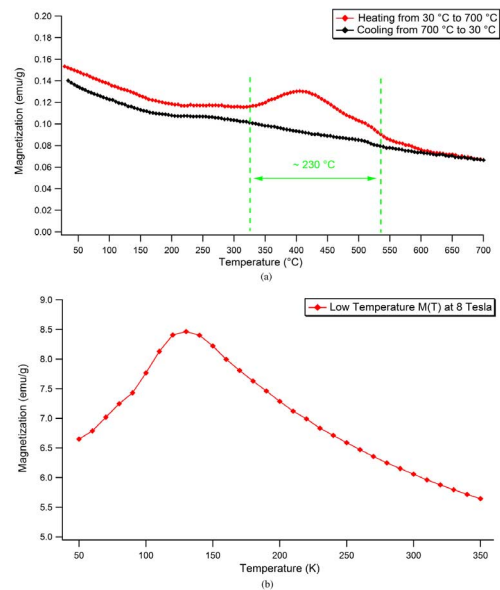

Fig. 4. (a) Change in magnetization with temperature from 300 °C to 700 °C with a ramp rate of 5 °C/min in an applied field of 3000 G. (b) Change in magnetization with temperature from 40 to 350 K in a field of 8 T ± 2 G.
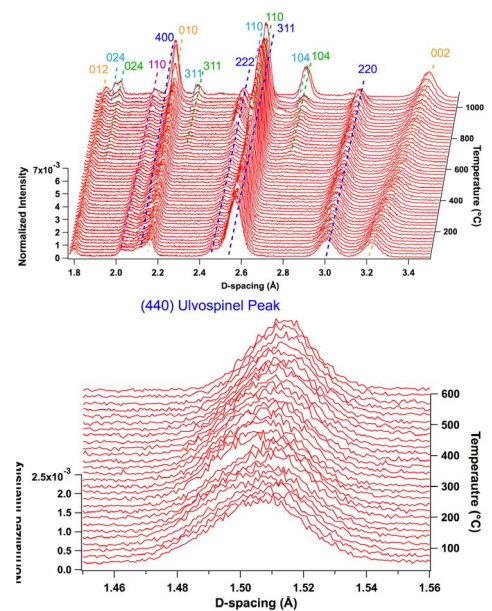

Fig. 5. (a) High T and P energy dispersive XRD results for ulvospinel. Waterfall plot shows Fe_2TiO_4 (dark blue), BCC α-Fe (purple), and BN (yellow) from the pressure cell. Above ~ 700 °C $FeTiO_3$ ilmenite (green) and ~ 1000 °C hematite (light blue) are observed. (b) Ulvospinel (440) peak from 300 °C to 600 °C.

of a second phase with a Néel temperature of 550 °C. The increase in magnetization occurs where diffusive processes are activated, and is attributed to titanomaghemitization [15], [22]. Titanomaghemitization refers to formation of metastable spinel $\gamma - (Fe, Ti)_2O_3$ that begins in the same temperature range where the XRD peak broadening is observed.

Fig. 4(b) illustrates the magnetic response of the sample in the large field of 8T (data taken on a PPMS magnetometer). This data shows textbook antiferromagnetic response below a Neel temperature of $\sim$120 K, which has been reported for ulvospinel. Paramagnetic response is observed above this temperature. The breadth of the $M(T)$ peak in high fields suggests distributed antiferromagnetic exchange interactions possibly arising from the random distribution of Ti^{4+} and Fe^{2+} cations on the octahedral B-sites of the spinel lattice. This suggests that high field experiments coupled with modeling of the distribution of exchange bonds may be of future interest. The titanomaghemitization, in Fig. 4(a), is a relatively small perturbation of the paramagnetic response of the ulvospinel, but sensitive magnetic measurements are capable of probing its progress. Fig. 4(b) shows low temperature $M(T)$ of ulvospinel. A peak in $M(T)$ (at 8T) occurs near 110 K, indicating the broad Neel transition temperature (T_N) of this synthesized ulvospinel. For $T > T_N$, ulvospinel is paramagnetic and its $M(T)$ obeys a Curie–Weiss law; for $T < T_N$, ulvospinel is antiferromagnetic and the increased magnetization with temperature is due to the spin rotation against exchange interaction which may be distributed [23].

High temperature and pressure energy dispersive XRD taken at the HPCAT 16 BM-B beamline at the APS are shown in the waterfall plot of Fig. 5. This data was taken on unannealed ulvospinel powder sample. The waterfall plot shows Fe_2TiO_4 ulvospinel peaks (dark blue), α-Fe peaks (purple), hexagonal BN (orange) and MgO (gray) peaks from the pressure cell. Above ~ 1000 °C hematite is observed (light blue). The phase transformations in the system are discussed below.

Transformation of the original ulvospinel solid solution with heating was observed in the data of Fig. 5(a) and broadening of

the spinel peaks above $\sim 300\,°\mathrm{C}$ (previously) attributed to titanomaghematization is observed to a substantially smaller degree. The suppression of the titanomaghemitization can be argued to be a result of the 650 MPa pressure used in this experiment (though the oxygen atmosphere in the cell is much less than in previous oxidizing experiments). Oxidation is known to take place by a vacancy assisted diffusive mechanism and the activation energy barrier for vacancy formation typically increases under pressure.

Chemical decomposition was observed at elevated temperatures. A small amount of unreacted Fe was observed, left from the synthesis process. Ilmenite peaks, indexed to the R-3m space group are shown to emerge at $\sim 700\,°\mathrm{C}$. Hematite peaks are observed near $\sim 1000\,°\mathrm{C}$. The appearance of hematite is not solely attributed to oxidation of this small amount of iron because the integrated intensity of the hematite peaks are larger than the original excess Fe peaks. Fig. 5(b) corresponds to the (440) peak, which shifts to higher d-spacing with increasing temperature and shows less dramatic broadening due to maghemitization, being affected both by lack of oxygen and pressure. This is observed for temperatures of $\sim 300° - 600\,°\mathrm{C}$ where ilmenite has not begun to form.

Ulvospinel peaks are observed to sharpen with increasing temperature. The (220) ulvospinel peak slightly shifts its peak position to a larger d-spacing due to thermal expansion. Some changes in peak width and intensity of the ulvospinel peaks are not yet fully understood. Changes of integrated intensity of ulvospinel peaks are observed, which is postulated to be caused by the structural changes from Fd-3m ulvospinel to R-3m ilmenite and formation of R-3m Fe_2O_3 (hematite) and will be the subject of future pressure dependent studies.

IV. Conclusion

The work of this study shows several atmosphere dependent transformations of ulvospinel, the end member of the titanomagnetite pseudo-binary system, with increase in temperature. Oxidation of the ulvospinel to form metastable titanomaghemite has been shown to occur at 300 $°\mathrm{C}$ in atmospheric conditions. Titanomaghematitzation was reduced in *in situ* heating experiments under higher pressures. Formation of ilmenite and hematite from ulvospinel was observed under high temperature, high pressure conditions.

Acknowledgment

References

[1] C. Klein and C. S. Hurlbut, *Manual of Mineralogy*, 21st ed. New York: Wiley, 1993.

[2] D. W. Strangeway, W. A. Gose, G. W. Pearce, and J. G. Cames, "Magnetism and the history of the moon," in *Proc. 18th Ann. Conf. Magn. Magn. Mater.*, 1973, pp. 1178–1197.

[3] D. Gubbins and E. Herrero-Bervera, *Encyclopedia of Geomagnetism and Paleomagnetism*. New York: Springer, 2007, Encyclopedia Earth Sci. Ser..

[4] G. Kletetschka, P. J. Wasilewski, and P. T. Taylor, "Mineralogy of the sources for magnetic anomalies on Mars," *Meteoritics Planetary Sci.*, vol. 35, pp. 895–899, 2000.

[5] P. Kearey and M. Brooks, *An Introduction to Geophysical Exploration*. New York: Blackwell, 1991.

[6] A. F. Buddington and D. H. Lindsley, "Iron-titanium oxide minerals and synthetic equivalents," *J. Petrol.*, vol. 5, pp. 310–357, 1964.

[7] J. M. D. Coey, S. Mørup, M. B. Madsen, and J. M. Knudsen, *J. Geophys. Res.*, vol. 95, p. 14423, 1990.

[8] A. T. Wise, M. Saenko, A. M. Velázquez, D. E. Laughlin, M. Diaz-Michelena, and M. E. McHenry, "Phase evolution in the $Fe_3O_4 - Fe_2TiO_4$ pseudo-binary system and its implications for remanent magnetization in Martian minerals," *IEEE Trans. Magn.*, vol. 47, pp. 4124–4127, 2011.

[9] R. Sanz, M. Cerdan, A. T. Wise, M. E. McHenry, and M. Diaz-Michelena, "Temperature dependent magnetization and remanent magnetization in pseudo-binary $(Fe2TiO4)_x - (Fe3O4)_{1-x}$ $(0.30 < x < 1.00)$ titanomagnetites," *IEEE Trans. Magn.*, vol. 47, pp. 4128–4131, 2011.

[10] M. Sorescu, T. Xu, A. Wise, M. Diaz-Michelena, and M. E. McHenry, "Studies on structural magnetic and thermal properties of $xFe_2TiO_4 - (1 - x)Fe_3O_4$ $(0 \le x \le 1)$ pseudo-binary system," *J. Magn. Magn. Mater.*, vol. 324, pp. 1453–1462, 2012.

[11] V. Raghavan, *Phase Diagrams of Ternary Iron Alloys*. Delhi, OH: ASM, 1987.

[12] P. Robinson, R. J. Harrison, S. A. McEnroe, and R. B. Hargraves, "Lamellar magnetism in the haematite-ilmenite series as an explanation for strong remanent magnetization," *Nature*, vol. 418, pp. 517–520, 2002.

[13] S. Akimoto, "Thermo-magnetic study of ferromagnetic minerals contained in igneous rocks," *J. Geomagnet. Geoelectr.*, vol. 6, pp. 1–14, 1954.

[14] L. Néel, "Some theoretical aspects of rock magnetism," *Adv. Phys.*, vol. 4, pp. 191–242, 1955.

[15] P. W. Readman and W. O'Reilly, "Magnetic properties of oxidized (cation deficient) titanomagnetites $(Fe, Ti, \Box)_3O_4$," *J. Geomagnet. Geoelectr.*, vol. 24, pp. 69–90, 1972.

[16] S. Lan, C. Groschner, J. Runco, A. Wise, M. Diaz-Michelena, D. E. Laughlin, and M. E. McHenry, "Phase identification and temperature-dependent magnetization of Ti-rich titanomagnetite $(0.5 \le x \le 1)$ in different atmospheres," *IEEE Trans. Magn.*, 2012, submitted for publication.

[17] M. A. Willard, Y. Nakamura, D. E. Laughlin, and M. E. McHenry, "Magnetic properties of ordered and disordered spinel-phase ferrimagnets," *J. Amer. Ceram. Soc.*, vol. 82, pp. 3342–3346, 1999.

[18] Y. Nakamura, P. A. Smith, D. E. Laughlin, M. J. De Graef, and M. E. McHenry, "Structure and magnetic properties of quenched $(Mn_xAl_{1-x})3O_4$ spinels and Hausmannites," *IEEE Trans. Magn.*, vol. 31, pp. 4154–4156, 1995.

[19] R. S. Carmichael, *Practical Handbook of Physical Properties of Rocks and Minerals*. Boca Raton, Fla: CRC Press, 1989.

[20] B. A. Wechsler, D. H. Lindsley, and C. T. Prewitt, "Crystal structure and cation distribution in titanomagnetites (Fe3-x,TixO4)," *Am. Mineral*, vol. 69, pp. 754–770, 1984.

[21] M. Ozima and N. Sakamoto, "Magnetic properties of titnomaghemite," *J. Geophys. Res.*, vol. 76, pp. 7035–7046, 1971.

[22] C. Keefer and P. Shive, "Curie temperature and lattice constant reference contours for synthetic titanomaghemites," *J. Geophys. Res.*, vol. 86, pp. 987–998, 1981.

[23] K. A. Gallagher, M. A. Willard, V. Zabenkin, D. E. Laughlin, and M. E. McHenry, "Distributed exchange interactions and temperature dependent magnetization in amorphous Fe88-xCoxZr7B4Cu1 alloys," *J. Appl. Phys.*, vol. 85, pp. 5130–5132, 1999.